The GTPase Rab3b/3c-positive recycling vesicles are involved in cross-presentation in dendritic cells

Liyun Zou, Jingran Zhou, Jinyu Zhang, Jingyi Li, Na Liu, Linlin Chai, Na Li, Ting Liu, Liqi Li, Zhunyi Xie, Hongli Liu, Ying Wan[1], and Yuzhang Wu[1]

Institute of Immunology, People's Liberation Army, Third Military Medical University, Chongqing 400038, China

Edited by Tak Wah Mak, Campbell Family Institute for Cancer Research, Ontario Cancer Institute, Princess Margaret Hospital, University Health Network, Toronto, Canada, and approved July 20, 2009 (received for review May 23, 2009)

Antigen cross-presentation in dendritic cells is a complex intracellular membrane transport process, but the underlying molecular mechanisms remain to be thoroughly investigated. In this study, we examined the effect of siRNA-mediated knockdown of 57 Rab GTPases, the key regulators of membrane trafficking, on antigen cross-presentation. Twelve Rab GTPases were identified to be associated with antigen cross-presentation, and Rab3b/3c was indicated to be colocalized with MHC class I molecules at perinuclear tubular structure. Tracing with fluorescence protein-tagged β_2-microglobulin demonstrated that the MHC class I molecules were internalized from the plasma membrane to Rab3b/3c-positive compartments, which were also colocalized with the internalized transferrin. Moreover, depletion of Rab3b/3c strongly reduced the fast phase recycling rate of transferrin receptors. Furthermore, the Rab3b/3c-positive compartments were colocalized with a fraction of Rab27a at a juxtaposition of phagosomes. Together, these data demonstrate that Rab3b/3c-positive recycling vesicles are involved in and may constitute one of the recycling compartments in exogenous antigen cross-presentation.

antigen presentation | membrane traffic | endosome

In classic MHC class I-restricted antigen presentation, foreign antigens are synthesized and processed within the cytosol for priming $CD8^+$ T cells. However, in some situations, such as the viral infection of epithelial cells and tumors, dendritic cells cannot synthesize foreign antigens in the cytosol. It has been suggested that dendritic cells present engulfed exogenous antigens in the context of MHC class I molecules for priming naive $CD8^+$ T cells. Early evidence of this process, now termed antigen cross-presentation, came from studies by Bevan (1, 2) on $CD8^+$ T-cell responses to an exogenous cellular antigen (minor histocompatibility antigens from transplanted cells). Over the past 30 years, antigen cross-presentation has been confirmed in vitro (3, 4) and has been supported by a series of experiments in vivo demonstrating that cross-presentation may play an important role in immunological tolerance and T-cell responses (5–7).

However, an obvious gap in the understanding of the intracellular mechanisms of antigen cross-presentation exists. Whereas engulfed exogenous antigens enter the endocytic system, the peptide-MHC class I molecule loading "machinery" involving transporter-associated with antigen presentation (TAP), tapasin, endoplasmic reticulum (ER) p57, calnexin, and calreticulin is located in the ER. Previous studies have shown that cross-presentation of numerous exogenous antigens is proteasome inhibitor sensitive and TAP dependent (8–11). One interpretation of these results is that these exogenous antigens are somehow translocated to the cytosol from the endosome, degraded by proteasomes, and loaded onto MHC class I molecules in the ER for presentation. Recent studies on the protein composition of the phagosome suggest that a part of the ER membrane fuses with a phagosome to form a unique compartment. The ER and phagosome contents in the compartment assemble local peptide-MHC class I molecule loading machinery for exogenous antigen cross-presentation (12, 13). However, a quantitative and dynamic study done by Touret et al. (14) failed to detect a significant contribution of the ER in forming or modifying phagosomes using a combination of biochemical, fluorescence imaging, and electron microscopy techniques.

Because cross-presentation is a continuous membrane transport process that begins from the endocytosis of an exogenous antigen and ends with the expression of MHC class I molecule-peptide complexes on the cell surface, a comprehensive analysis of membrane transport-related proteins involved in the process will facilitate a better understanding of antigen cross-presentation. Rab GTPases represent a large family of proteins that are recognized as key regulators of membrane trafficking. It has been found that specific and diverse Rab GTPases anchor to different vesicle membranes and recruit different effectors through their GDP/GTP binding, allowing them to switch and mediate intracellular membrane trafficking and organelle-targeted membrane fusion (15). In this study, we used ovalbumin (OVA)-expressing bacteria as particle antigens to test the effect of siRNA-mediated knockdown of 57 Rab GTPases, and thus identified 12 Rab proteins that are involved in antigen cross-presentation in dendritic cells. Among these Rab GTPases, we found that MHC class I molecules were enriched at Rab3b/3c-positive perinuclear tubular structures. Using ZsGreen-tagged β_2-microglobulin protein, we further identified the MHC class I molecules to be internalized from the plasma membrane to the Rab3b/3c-positive compartments. The recycling ligand transferrin was also internalized and enriched in the Rab3b/3c-positive vesicles. Moreover, the loss of Rab3b/3c by siRNA silencing reduced the fast phase recycling rates of transferrin receptors. Furthermore, the Rab3b/3c-positive compartments were colocalized with a fraction of Rab27a at a juxtaposition of phagosomes. These data identified a subset of recycling endosomes that are marked by Rab3b and Rab3c and are involved in and may constitute the recycling compartment of exogenous antigen cross-presentation.

Results

Identification of 12 Rab GTPases as Previously Undescribed Regulators of Cross-Presentation. After establishing a stable antigen cross-presentation assay for siRNA screening [supporting information (SI) Fig. S1], we constructed 171 lentivirus-based siRNA clones to 57 members of the mouse Rab family with the feline immunodeficiency virus (FIV) vector pFIV-Hl/U6 (the siRNA sequences are listed in Table S1). Because cross-presentation is sensitive to the number of antigen-presenting cells (APCs) (Fig. 1 *B* and *C*), we developed a simple and large-scale cell counting method as a part

Author contributions: L. Zou, J. Zhou, Y. Wan, and Y. Wu designed research; L. Zou, J. Zhou, J. Zhang, J. Li, N. Liu, L. Chai, N. Li, T. Liu, and Y. Wan performed research; L. Li, Z. Xie, H. Liu, and Y. Wan contributed new reagents/analytic tools; L. Zou, J. Zhou, J. Zhang, J. Li, L. Li, and Y. Wan analyzed data; and L. Zou, J. Zhou, and Y. Wan wrote the paper.

The authors declare no conflict of interest.

This article is a PNAS Direct Submission.

[1]To whom correspondence may be addressed. E-mail: wanying.cn@gmail.com or wuyuzhang@yahoo.com.

This article contains supporting information online at www.pnas.org/cgi/content/full/0905684106/DCSupplemental.

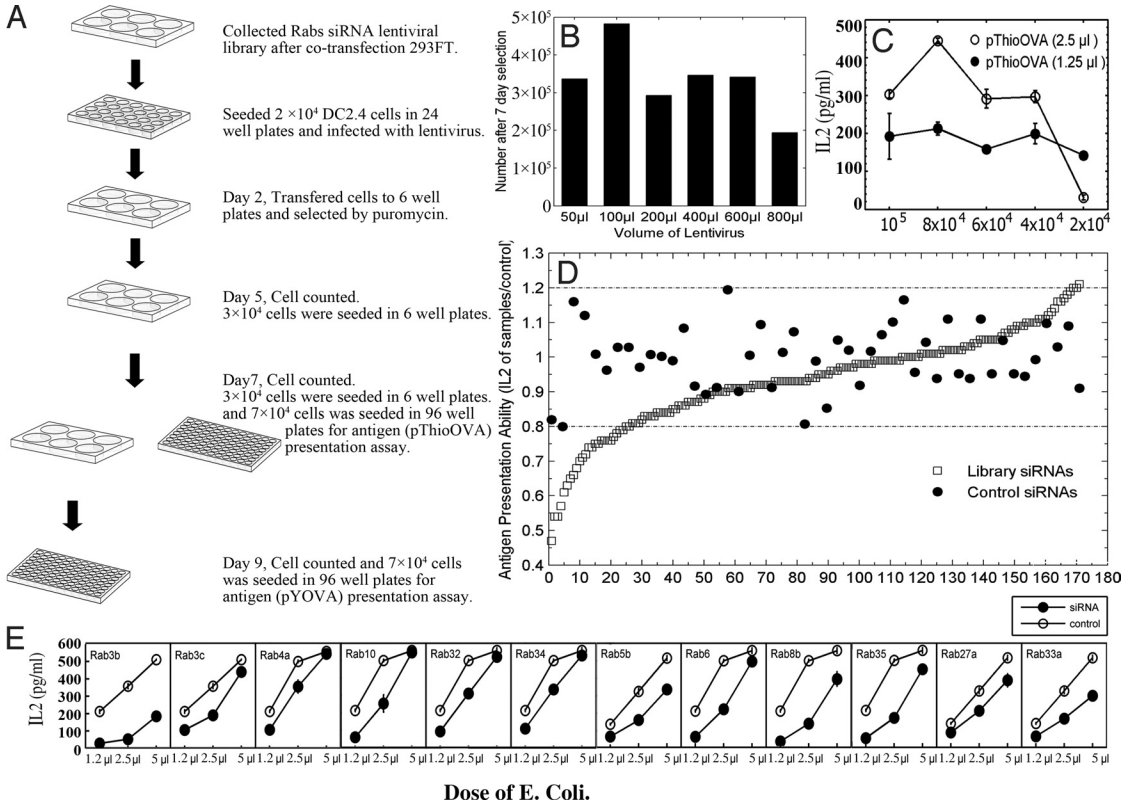

Fig. 1. Identification of the cross-presentation–associated Rab GTPases with lentivirus-based siRNA screening. (*A*) Scheme for identifying cross-presentation–related Rab GTPases by lentiviral-based siRNA. (*B*) Efficiency of lentivirus infection. DC2.4 cells were transfected with different titers of lentivirus for 24 h and subsequently cultured with puromycin (7 μg/mL) and counted after 7 days. (*C*) B3Z T-cell responses to different numbers of DC2.4 cells were analyzed after DC2.4 was prepulsed with 2.5 or 1.25 μL of *E. coli* BL21/pThio-OVA. (*D*) Antigen presentation ability scores of stably transfected dendritic cells. The antigen presentation ability score was the ratio of the IL-2 value of Rab siRNA stably transfected DC2.4 cells to the controls for each time of the antigen cross-presentation assay. The threshold ratio (0.8–1.2) was determined using 50 negative control data points (filled circles) from all screening processes (dash-dot line). Each open square represents 1 Rab siRNA stably transfected DC2.4 cell and is sorted in order of increasing antigen presentation ability scores. (*E*) B3Z response to DC2.4 cells containing siRNA against positive-screened Rab genes prepulsed with *E. coli* BL21/pThio-OVA at different doses.

of our loss-of-function RNA interference screening. The results of testing the effect of siRNA-mediated knockout of 57 Rab GTPases are shown in the screening flow chart in Fig. 1*A*. In brief, DC2.4 cells were seeded in 24-well plates and transduced with 200 μL of FIV (approximately 90 siRNA-expressing FIVs each time). After selection with puromycin in 6-well plates, wells with cell numbers greater than 3.0×10^4 were harvested at day 5 and designated as successfully transduced; otherwise, siRNA-expressing FIVs were repackaged until they met the designated requirements. Each stable siRNA-expressing DC2.4 population was seeded in 96-well plates twice for antigen presentation assays (Fig. 1*A*).

A scoring system for antigen presentation capacity was established by calculating the ratio of the IL-2 value of the Rab siRNA group to the controls. A threshold ratio was determined using 50 negative control datasets from all the screening processes. Our data showed that control FIV-transduced cells had a ratio of 0.8–1.2 (Fig. 1*D*, filled circles), whereas cells transduced with siRNA against various Rab genes had a ratio ranging from 0.40–1.21 (Fig. 1*D*, open squares). By this criterion, we identified 12 Rab GTPases as previously undescribed regulators of antigen cross-presentation in dendritic cells. Furthermore, after incubation with different doses of *Escherichia coli* BL21/thioredoxin (pThio) OVA, DC2.4 cells with stable expression of Rab3b, Rab5b, Rab8b, Rab27a, Rab33a, or Rab35 siRNA showed decreased antigen cross-presentation abilities regardless of the antigen dose. However, DC2.4 cells expressing siRNA against Rab3c, Rab4a, Rab6, Rab10, Rab32, or Rab34 appeared to have restored antigen cross-presentation ability when high doses of bacterial antigens were used (Fig. 1*E*).

To avoid off-target effects during siRNA screening (16, 17), 3 Stealth siRNAs (Invitrogen) were designed against each of the 12 Rab GTPases. Stealth siRNAs can eliminate sense strand off-target effects because Stealth RNAi modifications allow only the antisense strand to enter the RNAi pathway efficiently (18). Quantitative PCR analysis showed that 21 of the 36 siRNAs against these 12 Rab GTPases had reduced target gene expression by greater than 40% (Fig. S2*A*). At least 1 of 3 Stealth siRNAs against each of the 12 Rab GTPases inhibited antigen cross-presentation of transiently transfected DC2.4 cells (Fig. S2*B*). Thus, these data suggest that these 12 Rab GTPases are involved in antigen cross-presentation.

MHC Class I Molecules Were Enriched at Rab3b/3c-Positive Perinuclear Tubular Vesicles. To understand the potential mechanisms of these identified Rab GTPases in cross-presentation, we used red fluorescent protein-tagged (TagRFP) Rabs and yellow fluorescent protein-tagged (EYFP) MHC class I allele H2-K^b heavy chains to analyze the localization of these Rabs with MHC class I molecules. It has been previously shown that the fluorescence protein at the C-terminus of MHC class I molecules does not affect TAP association, assembly, or intracellular distribution of MHC class I molecules (19, 20). Interestingly, we found that a fraction of MHC class I molecules were significantly colocalized with Rab3b and Rab3c at perinuclear tubular vesicles (Fig. 2*A*). Immunofluorescent staining of the endogenous Rab3c confirmed the colocalization of the MHC class I molecules and Rab3c in perinuclear vesicles (Fig.

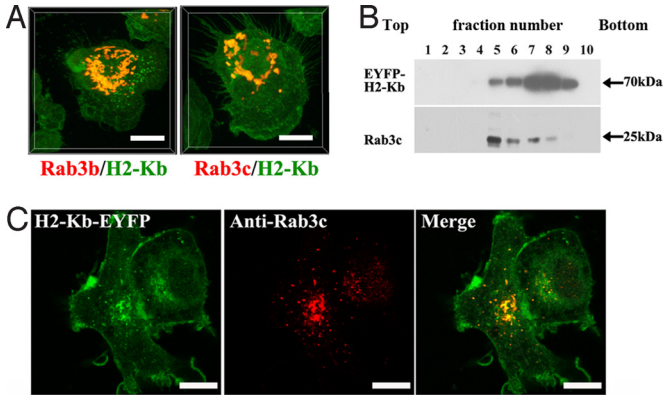

Fig. 2. The colocalization between MHC class I molecules and Rab3b/3c at perinuclear tubular vesicles. (*A*) After being stably transfected with TagRFP-Rab3b and -Rab3c and with EYFP–H2-K^b, DC2.4 cells were plated on coverslips and visualized using confocal microscopy. A stereo 3D rendering of collected confocal images shows the colocalization between Rab3b and Rab3c tubular vesicles (red) and H2-K^b molecules (green). (*B*) Distribution of Rab3c and EYFP–H2-K^b was analyzed by Western blotting after subcellular fractionation of EYFP–H2-K^b–expressing DC2.4 cells. (*C*) Colocalization between endogenous Rab3c and H2-K^b was analyzed by staining with rabbit anti-mouse Rab3c in EYFP–H2-K^b–expressing DC2.4 cells. (Scale bar: 10 μm.) These optically merged images are representative of at least 100 transduced cells examined by immunofluorescent confocal microscopy.

2*B*). Furthermore, Western blotting of proteins after subcellular fractionation by sucrose density gradient centrifugation provided evidence that a fraction of MHC class I molecules were sedimented in Rab3c-positive fractions (Fig. 2*C*). Because Rab3b and Rab3c are located on the same vesicles (21) (Fig. S3) and have been well defined as exocytosis-associated Rabs, our data show that a fraction of intracellular MHC class I molecules were enriched at Rab3b/3c-positive perinuclear tubular vesicles, which are most likely one type of compartment related to exocytosis.

Internalized MHC Class I Molecules Were Transported to Rab3b/3c-Positive Vesicles. Because the efflux of biosynthesized MHC class I molecules is mainly from the ER to the Golgi, we assessed the effects of brefeldin A (BFA) on the storage of H2-K^{b}YFP in Rab3b/3c-positive vesicles. The H2-K^{b}YFP on cell surface membranes disappeared after incubation with BFA for 4 h. However, the concentration of H2-K^{b}YFP in the Rab3b/3c-positive vesicles did not show any apparent change on BFA treatment (Fig. 3 *A* and *B*). ER staining with calnexin also showed that Rab3b/3c vesicles had little overlap with ER (Fig. S4). These results indicate that MHC class I molecules in Rab3b/3c-positive vesicles are not directly derived from the biosynthetic protein secretory pathway.

Because β_2-microglobulin can be used specifically to track the internalized MHC class I molecules (22), we prepared ZsGreen-tagged β_2-microglobulin in an eukaryotic expression system. Using a TAP-deficient cell line, we confirmed that the ZsGreen-tagged β_2-microglobulin was specifically bound to the cell surface MHC class I molecules (Fig. S5). Incubation of ZsGreen-tagged β_2-microglobulin proteins with DC2.4 cells showed the colocalization of internalized β_2-microglobulin and Rab3b/3c-positive vesicles (Fig. 3*D*). Quantification of relative fluorescence intensity of subcellular fractions using sucrose density gradient centrifugation also indicated that ZsGreen-tagged β_2-microglobulin proteins were enriched at the TagRFP-Rab3b/3c fractions (Fig. 3*C*). Time-lapse observation with spinning disk confocal microscopy revealed that ZsGreen-tagged β_2-microglobulin–positive vesicles were tethered and fused to Rab3b/3c-positive vesicles (Movies S1 and S2). These data suggest that cell surface MHC class I molecules can be internalized and transported to the Rab3b/3c-positive vesicles.

Rab3b/3c-Positive Vesicles Represent Perinuclear Recycling Endosomes Adjacent to Phagosomes. To characterize the Rab3b/3c-positive vesicles further, we examined the distribution and recycling of FITC-transferrin after incubation with DC2.4 cells. After incubating dendritic cells with FITC-transferrin, we observed that some internalized transferrin was enriched at perinuclear tubular structures of Rab3b- or Rab3c-positive vesicles (Fig. 4*A* and Fig. S6*A*). The colocalization between Rab3b/3c and transferrin in dendritic cells prompted us to examine whether Rab3b/3c controls the recycling pathway of transferrin. At least 2 distinct pathways have been described in transferrin receptor recycling. One pathway directly from sorting endosomes has a rapid time course, whereas the slow pathway involves the endocytic recycling compartment, which is a collection of perinuclear tubular organelles (23). We loaded dendritic cells with fluorescently labeled transferrin for 30 min and measured the kinetics of chase after transfer into media containing unlabeled transferrin. Quantification of intracellular FITC-labeled transferrin by FACS cytometry revealed that the rapid recycling rates, as measured after a 5- to 20-min chase, appeared strongly reduced in stable Rab3b/3c-silenced dendritic cells (Fig. 4 *B* and *C*), suggesting that Rab3b/3c is involved in the rapid recycling pathway. Furthermore, with a series of EYFP-Rabs, we observed the colocalization between Rab3b/3c and other identified cross-presentation–associated Rabs. To our surprise, most of the identified Rabs, such as Rab5b, Rab8b, Rab10, Rab33a, Rab34, and Rab35, were localized in Rab3b/3c vesicles (Fig. S7). Interestingly, a fraction of Rab8b, Rab10, Rab34, and Rab35 was also associated with the plasma membrane (Fig. S7). Among these Rabs, Rab8b, Rab10, and Rab35 were reported to control a recycling transport step from endosomal compartments to the plasma membrane (24–26). Our findings demonstrate the cooperation of these Rabs in controlling a specific recycling pathway from endosomes to the plasma membrane in dendritic cell cross-presentation.

To establish the role of the Rab3b/3c vesicles in cross-presentation further, we observed the relation between these vesicles and phagosomes using enhanced cyan fluorescent protein (ECFP)-expressing *E. coli* as a particle exogenous antigen. After incubating DC2.4 cells with *E. coli* for 4 h, 3D reconstruction images were produced. It can be clearly visualized that a part of the intracellular Rab3b- and H2-K^{b}YFP–positive compartment was localized in the juxtaposition of internalized *E. coli* (Fig. 5*A*). Similar images were also obtained in Rab3c and H2-K^{b}YFP stably transfected dendritic cells (Fig. S6*B*). Because it has been recently reported that Rab27a-deficient dendritic cells demonstrated a defect in cross-presentation because Rab27a was recruited to phagosomes to limit the degradation of ingested particles (27), we examined the colocalization between Rab27a and Rab3b/3c. To our surprise, a fraction of Rab27a was colocalized with Rab3b and Rab3c at a compartment closely adjacent to phagosomes (Fig. 5*B* and Fig. S6*C*). Our data characterize the Rab3b/3c-positive vesicles as perinuclear recycling endosomes that are adjacent to phagosomes during phagocytosis.

Discussion

Much effort has been put into identifying antigen cross-presentation–related genes, such as TAP, Nox2, and Rac1 (13, 27, 28), which provide important clues for understanding the cellular mechanism of this important antigen presentation pathway. However, there is little information at present about the membrane transport participators in cross-presentation. Recently, RNAi-based gene silencing has emerged as a powerful approach for reverse functional genomics. Many groups have used siRNA screening to identify genes involved in comprehensive physiological phenomena (29). In this study, we achieved stable gene silencing in dendritic cell line DC2.4 using a lentivirus approach. Twelve Rab genes were identified as associated with cross-presentation of dendritic cells, including Rab3b, Rab3c, Rab4a, Rab5b, Rab6, Rab8b, Rab10, Rab27a, Rab32, Rab33a, Rab34, and Rab35.

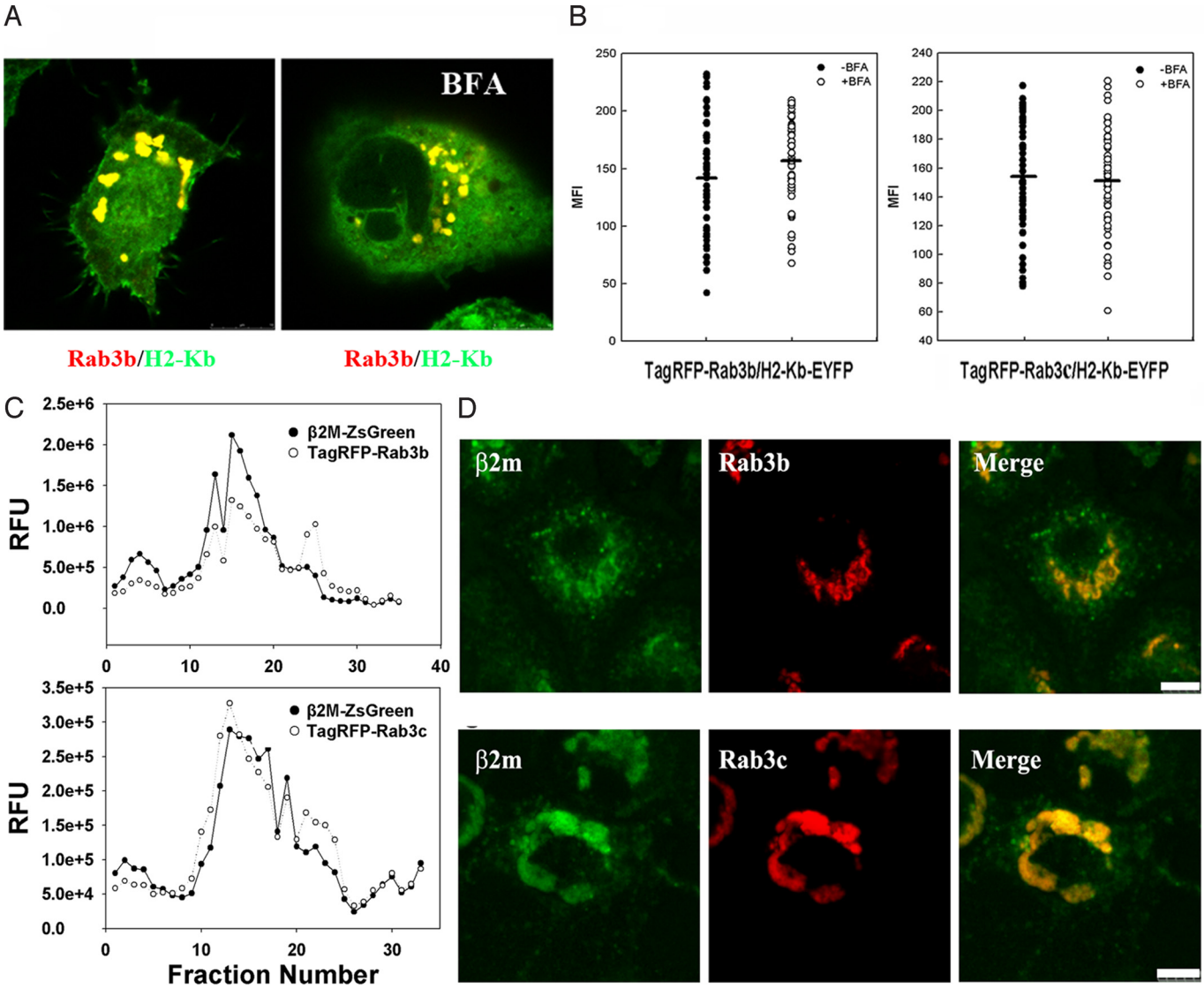

Fig. 3. Transporting the internalized MHC class I molecules to Rab3b/3c-positive vesicles. (*A*) Stably transfected DC2.4 cells were incubated with media or 10 μg/mL BFA for 4 h. The confocal images revealed that the concentration of MHC class I molecules (green) in Rab3b/3c-positive vesicles (red) is resistant to BFA treatment. (*B*) Quantitative analysis of the mean fluorescence intensity of EYFP–H2-K^b in Rab3b/3c-positive vesicles with or without BFA treatment. Each symbol represents an individual Rab3b/3c-positive vesicle. Small horizontal lines indicate the mean. (*C*) β_2-Microglobulin–ZsGreen fusion proteins were incubated with stable transfected TagRFP-Rab3b or TagRFP-Rab3c dendritic cells for 30 min on ice, and cells were then washed and warmed to 37 °C for 1 h. The distribution of TagRFP-Rab3b/3c and β_2-microglobulin–ZsGreen fusion proteins was analyzed by fluorescence intensity measurement after subcellular fractionation. (*D*) Confocal images of stably transduced DC2.4 cells pulsed with β_2-microglobulin–ZsGreen fusion proteins. These optically merged images are representative of at least 100 transduced cells examined by immunofluorescent confocal microscopy. Yellow indicates colocalization of green and red. (Scale bar: 10 μm.)

According to current data on Rabs, these cross-presentation–related Rab GTPases may be arbitrarily classified into an endocytosis group and an exocytosis group. Some Rabs (Rab4a, Rab5b, Rab8b, Rab10, Rab27a, Rab32, Rab34, and Rab35) have been reported as components of phagosomes after quantitative proteomic assays or microscope observation with fluorescent protein-tagged Rabs (30, 31). Our data also showed the recruitment of these Rabs to phagosomes during phagocytosis (Fig. S8*A*). On the other hand, the role of Rabs (Rab3b, Rab3c, Rab4a, Rab6, Rab27a, Rab32, Rab34, and Rab35) has been investigated in different exocytotic pathways. Rabs (Rab3b and Rab3c) also regulate secretory vesicle traffic in neurons and endocrine cells (32). Rabs (Rab4a and Rab35) are required for recycling from the early endosomes to the plasma membrane (15, 26). Rabs (Rab27a and Rab32) are involved in exocytosis of lysosome-related organelles, such as melanosomes (33, 34). Rabs (Rab6 and Rab34) have been morphologically associated with the Golgi complex and are thought to be regulators in the exocytosis of the Golgi to the plasma membrane (35, 36). Our findings therefore suggest that a complex membrane transport mechanisms govern the antigen cross presentation process.

Although engulfed exogenous antigens enter the endocytic system for cross-presentation, the origin and function of the endosomal MHC class I molecules are unclear. A role of these endosomal MHC class I molecules in cross-presentation has been suggested by several researchers. MHC class I molecules have been found in great number in MHC class II-containing endosomes of dendritic cells (37). The TAP inhibitor that was selectively delivered into early endosomes has been shown to impair the cross-presentation of soluble antigens (38). The tyrosine-based targeting signals at the MHC class I cytoplasmic domain direct MHC class I molecules to LAMP-1–positive compartments and regulate cross-presentation

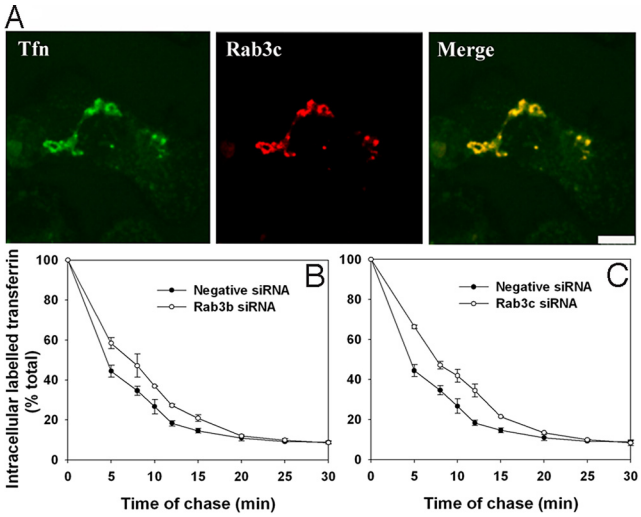

Fig. 4. Rab3c is localized at recycling endosomes and controls a rapid recycling transport step of the transferrin receptor. (*A*) TagRFP-Rab3c–expressing DC2.4 cells were pulsed with FITC-Tfn and viewed under confocal microscopy. Images revealed the colocalization of FITC-Tfn (green) with Rab3c-positive vesicles (red). (*B*, *C*) DC2.4 cells stably silencing Rab3b (*B*) or Rab3c (*C*) were incubated with FITC-Tfn for 1 h at 37 °C. Transferrin receptor recycling to the cell surface was measured by quantification of intracellular FITC-Tfn after different chase times. The results are expressed as percentages of initial FITC-transferrin (mean ± SEM, $n = 3$, >8,000 cells were analyzed by cytometry for each time point).

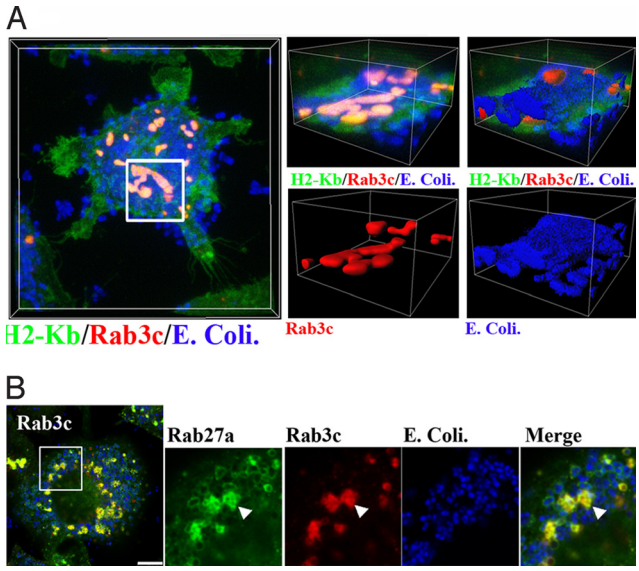

Fig. 5. Rab3c was colocalized with a fraction of Rab27a at a juxtaposition of phagosomes. (*A*) Stably transfected DC2.4 cells were incubated with *E. coli* BL21/pECFP-OVA for 4 h. Coverslips were mounted on slides and detected by confocal microscopy. Stereo 3D rendering of collected confocal images shows that Rab3c tubular vesicles (red) colocalize with H2-K^b molecules (green) at a juxtaposition of phagosomes. (*B*) DC2.4 transfected with EYFP-Rab27a and TagRFP-Rab3c lentivirus. After incubation with *E. coli* BL21/pECFP-OVA, confocal images reveal that Rab3c tubular vesicles (red) colocalize with Rab27a molecules (green) at a juxtaposition of phagosomes. Enlarged images show the phagosomes and concentrated compartments (arrowheads) after engulfment. These optically merged images are representative of at least 100 transduced cells by immunofluorescent confocal microscopy. (Scale bar: 10 μm.)

in antiviral immunity (39). In the study, we have revealed that a fraction of internalized MHC class I molecules from plasma membrane accumulate in the Rab3b/3c-positive compartments at the juxtaposition of internalized bacteria. Characterization of the vesicles demonstrates that the rapid recycling of transferrin receptors is under the control of Rab3b/3c in dendritic cells. Moreover, the impairment of cross-presentation after knockout of Rab3b/3c suggests that Rab3b/3c plays an important role in the recycling of internalized MHC class I molecules during cross-presentation. Because Rab3a–Rab3d are well-defined regulators of secretory vesicle traffic (32), Rab3b/3c-positive recycling endosomes may contribute to the exocytotic step of antigen cross-presentation.

The endocytic system consisted of a dynamic network of organelles characterized by different biochemical composition and functional diversity. A series of Rabs has been reported to serve as regulators in transport of the endosomal system. Recently, it has been reported that Rab27a is involved in transport of NADPH oxidase Nox2 to phagosomes (27), which causes alkalinization of phagosomes to promote cross-presentation of particle antigens in dendritic cells (40, 41). Rab27a has been discovered to cause pigmentary dilution and immunodeficiency in humans with Griscelli syndrome. Moreover, Rab27a is involved in the exocytic transport of lysosome-related organelles, such as melanosomes in melanocytes and lytic granules in cytotoxic T lymphocytes (42). In this study, the recruitment of Rab27a to phagosomes is similar to previous observations (40). The most interesting outcome is that a fraction of Rab27a that is not recruited to phagosomes is concentrated and colocalized with Rab3b/3c (Fig. 5). A similar observation has recently been made that Rab3a and Rab27a are present on secretory vesicles and cooperatively regulate the docking step of vesicle exocytosis in neuroendocrine PC12 cells (43). The adjacent nature of phagosomes to Rab3b/3c- and Rab27a-positive compartments suggests a transport link between the phagosomes and Rab3b/3c-positive recycling endosomes.

In summary, our data show that internalized MHC class I molecules accumulate in the Rab3b/3c-positive recycling endosomes, which colocalize with Rab27a at the juxtaposition of phagosomes and are involved in cross-presentation. The results provide a proposed model for the membrane transport process of cross-presentation as indicated in Fig. S8*B*, in which the Rab3b/3c-positive recycling endosomes contribute to the exocytic step of exogenous antigen cross-presentation. Further investigations on the transport mechanisms between phagosomes and these recycling endosomes in cross-presentation may provide opportunities to develop unique immunotherapeutic strategies.

Materials and Methods

Cell Culture and Lentivirus Production. The murine dendritic cell line DC2.4 was kindly provided by Dr. K. Rock (Dana Farber Cancer Institute, Boston, Massachusetts), grown in RPMI 1640 with 10% (vol/vol) FBS, and supplemented with 50 μM β_2-mercaptoethanol (4). B3Z, a T-cell hybridoma cell line specific for the $OVA_{257-264}$ peptide (SIINFEKL) in the context of K^b, was a gift from Dr. N. Shastri (University of California, Berkeley, CA). B3Z cells were maintained in RPMI medium 1640 supplemented with 10% (vol/vol) FBS, 50 μM β_2-mercaptoethanol, penicillin (200 U/mL), and streptomycin (200 μg/mL) (44, 45). The 293FT cell line (Invitrogen) was maintained in DMEM supplemented with 10% (vol/vol) FBS.

Lentivirus particles derived from FIV were produced by transient cotransfected lentiviral expression constructs into 293FT cells with the pFIV-PACK Lentiviral Packaging Kit (System Biosciences) following the $Ca_3(PO4)_2$ transfection protocol. Similarly, the production of HIV replication-incompetent lentiviral particles was accomplished by simultaneously delivering lentiviral transfer vectors and packaging plasmids (psPAX2 and pMG2.D, kindly provided by Trono Lab) into 293FT cells. Pseudoviral particles generated by 293FT cells were frozen within 48 h and used in later experiments.

MHC Class I Molecule-Restricted Presentation Assay and Cell Count. For cross-presentation, 7.0×10^4 FIV stably transduced dendritic cells were seeded in 96-well plates. Bacterial antigens were added to the APCs and coincubated for 4 h at 37 °C (for details of bacterial antigens, refer to Fig. S1). Antigen processing was then stopped by fixing the cells in 1% paraformaldehyde for 15 min. After washing 5 times with HBSS, 5.0×10^4 B3Z T-hybridoma cells were added for 20 h of incubation. IL-2 production by the T-cell hybridoma cells was quantified using an IL-2 ELISA kit (BD PharMingen).

For large-scale counting of APC numbers in the siRNA library screen process,

IMMUNOLOGY

1.0×10^8 DC2.4 cells were stained with 5,6-carboxy-succinimidyl-fluorescein-ester (CFSE). Next, 100 μL of unstained transduced cell samples was mixed with 100 μL (1.0×10^6) of CFSE-stained cells and analyzed by flow cytometry. Cell numbers were calculated using a standard curve from a serial dilution of a known concentration of unstained DC2.4 cell samples.

Fluorescent Rab Constructs and β_2-Microglobulin–ZsGreen Fusion Protein Purification. To construct fluorescent protein-tagged Rab, PCR primers with restriction enzyme sites were designed for amplification of full-length Rab fragments from cDNA vectors (Open Biosystems). The H2-K^b and β_2-microglobulin cDNA fragments with appropriate restriction endonuclease sites were amplified by reverse transcriptase PCR from DC2.4 RNA and confirmed with sequencing. EYFP-Rabs, TagRFP-Rabs, H2-K^b–EYFP, and β_2-microglobulin–ZsGreen constructs were cloned into modified FUGW vectors (kindly provided by Dr. David Baltimore, California Institute of Technology, Pasadena, California) (46, 47).

β_2-microglobulin–ZsGreen fusion proteins were purified with nickel affinity chromatography after large-scale transfection into 293FT cells using $Ca_3(PO4)_2$. Briefly, 1×10^7 293FT cell pellets were resuspended in 20 mL of ice-cold lysis buffer (50 mM NaH_2PO_4, 300 mM NaCl, 10 mM imidazole, 1% Nonidet P-40, and protease inhibitor mixture) and sonicated 5 times for 30 s on ice, followed by centrifugation at $15,000 \times g$ for 20 min at 4 °C. The supernatant was loaded into the Ni-NTA superflow column (QIAGEN, GmbH) and eluted with imidazole. β_2-microglobulin–ZsGreen fusion proteins finally concentrated in PEG8000 to 0.2 mg/mL and were stored at 4 °C in PBS.

Sucrose Density Gradient Fractionation and Western Blot Analysis. A total of 2×10^7 cells were homogenized, and intact cells and nuclei were removed by centrifugation. The supernatant was loaded onto a premade sucrose gradient consisting of 1-mL layers of 10, 20, 30, 40, 55, and 60% (wt/vol), sucrose in 10 mM Hepes buffer. Gradients were centrifuged in an SW55 rotor at 1 h at $100,000 \times g$ at 4 °C, after which 200-μL fractions were collected from top to bottom. Proteins in each fraction were subjected to Western blot analysis or fluorescence intensity measurement by a Beckman Coulter Paradigm Detection Platform.

Measurement of Transferrin Recycling. Dendritic cells were preincubated in serum-free medium (RPMI 1640/0.6% BSA) for 20 min to remove any residual transferrin and were then exposed to 10 μg/mL FITC-transferrin (Invitrogen) for 1 h at 37 °C. After transferrin internalization, the cells were washed with ice-cold PBS/0.1% BSA to remove unbound transferrin and were chased in complete RPMI 1640/0.5% BSA, 600 μg/mL unlabeled transferrin, and 50 μM deferoxamine (Sigma) at 37 °C. At the end of each chase time point, cell surface-bound fluorescent transferrin was removed with an acid wash in PBS/0.1% BSA and 25 mM glacial acetic acid (pH 4.2), followed by a wash with PBS/0.1% BSA (pH 7.0), and the cells were detached from the wells with trypsin and subsequently fixed in cold 1% paraformaldehyde. Recycling was then measured as the loss of cell-associated fluorescence by flow cytometry.

Additional materials and methods can be found in *SI Materials and Methods*.

ACKNOWLEDGMENTS. We thank Dr. K. Rock for kindly providing the dendritic cell line DC2.4 and Dr. N. Shastri for the T-cell hybridoma B3Z. We express our gratitude to Wei Sun, Liting Wang, Xiaolan Fu, and Qing Ji for their technical assistance. We are grateful to Dr. Jennifer E. Hobbs, Jianxun Song, and Liwei Lu for critical reading of the manuscript. This work was supported by a grant-in-aid from the National Basic Research Program of China (973 program, 2010CB911800 and 2007CB512401) and the National Natural Science Foundation of China (30400392, 30490241, and 30871224).

1. Bevan MJ (1976) Cross-priming for a secondary cytotoxic response to minor H antigens with H-2 congenic cells which do not cross-react in the cytotoxic assay. *J Exp Med* 143:1283–1288.
2. Bevan MJ (2006) Cross-priming. *Nat Immunol* 7:363–365.
3. Reis e Sousa C, Germain RN (1995) Major histocompatibility complex class I presentation of peptides derived from soluble exogenous antigen by a subset of cells engaged in phagocytosis. *J Exp Med* 182:841–851.
4. Shen Z, Reznikoff G, Dranoff G, Rock KL (1997) Cloned dendritic cells can present exogenous antigens on both MHC class I and class II molecules. *J Immunol* 158:2723–2730.
5. Lenz LL, Butz EA, Bevan MJ (2000) Requirements for bone marrow-derived antigen-presenting cells in priming cytotoxic T cell responses to intracellular pathogens. *J Exp Med* 192:1135–1142.
6. Sigal LJ, Crotty S, Andino R, Rock KL (1999) Cytotoxic T-cell immunity to virus-infected non-haematopoietic cells requires presentation of exogenous antigen. *Nature* 398:77–80.
7. Sigal LJ, Rock KL (2000) Bone marrow-derived antigen-presenting cells are required for the generation of cytotoxic T lymphocyte responses to viruses and use transporter associated with antigen presentation (TAP)-dependent and -independent pathways of antigen presentation. *J Exp Med* 192:1143–1150.
8. Garin J, et al. (2001) The phagosome proteome: Insight into phagosome functions. *J Cell Biol* 152:165–180.
9. Rodriguez A, Regnault A, Kleijmeer M, Ricciardi-Castagnoli P, Amigorena S (1999) Selective transport of internalized antigens to the cytosol for MHC class I presentation in dendritic cells. *Nat Cell Biol* 1:362–368.
10. Huang AY, Bruce AT, Pardoll DM, Levitsky HI (1996) In vivo cross-priming of MHC class I-restricted antigens requires the TAP transporter. *Immunity* 4:349–355.
11. Kovacsovics-Bankowski M, Rock KL (1995) A phagosome-to-cytosol pathway for exogenous antigens presented on MHC class I molecules. *Science* 267:243–246.
12. Houde M, et al. (2003) Phagosomes are competent organelles for antigen cross-presentation. *Nature* 425:402–406.
13. Guermonprez P, et al. (2003) ER-phagosome fusion defines an MHC class I cross-presentation compartment in dendritic cells. *Nature* 425:397–402.
14. Touret N, et al. (2005) Quantitative and dynamic assessment of the contribution of the ER to phagosome formation. *Cell* 123:157–170.
15. Zerial M, McBride H (2001) Rab proteins as membrane organizers. *Nat Rev Mol Cell Biol* 2:107–117.
16. Jackson AL, et al. (2003) Expression profiling reveals off-target gene regulation by RNAi. *Nat Biotechnol* 21:635–637.
17. Echeverri CJ, Perrimon N (2006) High-throughput RNAi screening in cultured cells: A user's guide. *Nat Rev Genet* 7:373–384.
18. Smith C (2006) Sharpening the tools of RNA interference. *Nat Methods* 3:475–486.
19. Marguet D, et al. (1999) Lateral diffusion of GFP-tagged H2Ld molecules and of GFP-TAP1 reports on the assembly and retention of these molecules in the endoplasmic reticulum. *Immunity* 11:231–240.
20. Gromme M, et al. (1999) Recycling MHC class I molecules and endosomal peptide loading. *Proc Natl Acad Sci USA* 96:10326–10331.
21. Iezzi M, et al. (1999) Subcellular distribution and function of Rab3A, B, C, and D isoforms in insulin-secreting cells. *Mol Endocrinol* 13:202–212.
22. Chiu I, Davis DM, Strominger JL (1999) Trafficking of spontaneously endocytosed MHC proteins. *Proc Natl Acad Sci USA* 96:13944–13949.
23. Maxfield FR, McGraw TE (2004) Endocytic recycling. *Nat Rev Mol Cell Biol* 5:121–132.
24. Babbey CM, et al. (2006) Rab10 regulates membrane transport through early endosomes of polarized Madin-Darby canine kidney cells. *Mol Biol Cell* 17:3156–3175.
25. Chen S, Liang MC, Chia JN, Ngsee JK, Ting AE (2001) Rab8b and its interacting partner TRIP8b are involved in regulated secretion in AtT20 cells. *J Biol Chem* 276:13209–13216.
26. Kouranti I, Sachse M, Arouche N, Goud B, Echard A (2006) Rab35 regulates an endocytic recycling pathway essential for the terminal steps of cytokinesis. *Curr Biol* 16:1719–1725.
27. Jancic C, et al. (2007) Rab27a regulates phagosomal pH and NADPH oxidase recruitment to dendritic cell phagosomes. *Nat Cell Biol* 9:367–378.
28. Luckashenak N, et al. (2008) Constitutive crosspresentation of tissue antigens by dendritic cells controls CD8+ T cell tolerance in vivo. *Immunity* 28:521–532.
29. Chen M, Du Q, Zhang HY, Wang X, Liang Z (2007) High-throughput screening using siRNA (RNAi) libraries. *Expert Rev Mol Diagn* 7:281–291.
30. Smith AC, et al. (2007) A network of Rab GTPases controls phagosome maturation and is modulated by Salmonella enterica serovar Typhimurium. *J Cell Biol* 176:263–268.
31. Rogers LD, Foster LJ (2007) The dynamic phagosomal proteome and the contribution of the endoplasmic reticulum. *Proc Natl Acad Sci USA* 104:18520–18525.
32. Darchen F, Goud B (2000) Multiple aspects of Rab protein action in the secretory pathway: Focus on Rab3 and Rab6. *Biochimie* 82:375–384.
33. Izumi T (2007) Physiological roles of Rab27 effectors in regulated exocytosis. *Endocr J* 54:649–657.
34. Wasmeier C, et al. (2006) Rab38 and Rab32 control post-Golgi trafficking of melanogenic enzymes. *J Cell Biol* 175:271–281.
35. Grigoriev I, et al. (2007) Rab6 regulates transport and targeting of exocytotic carriers. *Dev Cell* 13:305–314.
36. Goldenberg NM, Grinstein S, Silverman M (2007) Golgi-bound Rab34 is a novel member of the secretory pathway. *Mol Biol Cell* 18:4762–4771.
37. MacAry PA, et al. (2001) Mobilization of MHC class I molecules from late endosomes to the cell surface following activation of CD34-derived human Langerhans cells. *Proc Natl Acad Sci USA* 98:3982–3987.
38. Burgdorf S, Scholz C, Kautz A, Tampe R, Kurts C (2008) Spatial and mechanistic separation of cross-presentation and endogenous antigen presentation. *Nat Immunol* 9:558–566.
39. Lizee G, et al. (2003) Control of dendritic cell cross-presentation by the major histocompatibility complex class I cytoplasmic domain. *Nat Immunol* 4:1065–1073.
40. Savina A, et al. (2006) NOX2 controls phagosomal pH to regulate antigen processing during crosspresentation by dendritic cells. *Cell* 126:205–218.
41. Mantegazza AR, et al. (2008) NADPH oxidase controls phagosomal pH and antigen cross-presentation in human dendritic cells. *Blood* 112:4712–4722.
42. Fukuda M (2005) Versatile role of Rab27 in membrane trafficking: Focus on the Rab27 effector families. *J Biochem* 137:9–16.
43. Tsuboi T, Fukuda M (2006) Rab3A and Rab27A cooperatively regulate the docking step of dense-core vesicle exocytosis in PC12 cells. *J Cell Sci* 119:2196–2203.
44. Shastri N, Gonzalez F (1993) Endogenous generation and presentation of the ovalbumin peptide/Kb complex to T cells. *J Immunol* 150:2724–2736.
45. Karttunen J, Sanderson S, Shastri N (1992) Detection of rare antigen-presenting cells by the lacZ T-cell activation assay suggests an expression cloning strategy for T-cell antigens. *Proc Natl Acad Sci USA* 89:6020–6024.
46. Merzlyak EM, et al. (2007) Bright monomeric red fluorescent protein with an extended fluorescence lifetime. *Nat Methods* 4:555–557.
47. Lois C, Hong EJ, Pease S, Brown EJ, Baltimore D (2002) Germline transmission and tissue-specific expression of transgenes delivered by lentiviral vectors. *Science* 295:868–872.